



Tissue variations of mosaic genome-wide paternal uniparental disomy and phenotype of multi-syndromal congenital hyperinsulinism

Christesen, Henrik Thybo; Christensen, Lene Gaarsmand; Löfgren, Åsa Mattsson; Brøndum-Nielsen, Karen; Svensson, Johan; Brusgaard, Klaus; Samuelsson, Sofie; Elfving, Maria; Jonson, Tord; Grønskov, Karen; Rasmussen, Lars; Backman, Torbjörn; Hansen, Lars Kjaersgaard; Larsen, Annette Rønholt; Petersen, Henrik; Detlefsen, Sönke

Published in:

European Journal of Medical Genetics

DOI:

[10.1016/j.ejmg.2019.02.004](https://doi.org/10.1016/j.ejmg.2019.02.004)

Publication date:

2020

Document version

Publisher's PDF, also known as Version of record

Document license:

[CC BY-NC-ND](#)

Citation for published version (APA):

Christesen, H. T., Christensen, L. G., Löfgren, Å. M., Brøndum-Nielsen, K., Svensson, J., Brusgaard, K., Samuelsson, S., Elfving, M., Jonson, T., Grønskov, K., Rasmussen, L., Backman, T., Hansen, L. K., Larsen, A. R., Petersen, H., & Detlefsen, S. (2020). Tissue variations of mosaic genome-wide paternal uniparental disomy and phenotype of multi-syndromal congenital hyperinsulinism. *European Journal of Medical Genetics*, 63(1), [103632]. <https://doi.org/10.1016/j.ejmg.2019.02.004>



Tissue variations of mosaic genome-wide paternal uniparental disomy and phenotype of multi-syndromal congenital hyperinsulinism

Henrik Thybo Christesen^{a,b,c,*,1}, Lene Gaarsmand Christensen^{d,1}, Åsa Mattsson Löfgren^e, Karen Brøndum-Nielsen^f, Johan Svensson^g, Klaus Brusgaard^{c,h}, Sofie Samuelssonⁱ, Maria Elfving^{j,k}, Tord Jonsonⁱ, Karen Grønskov^f, Lars Rasmussen^l, Torbjörn Backman^m, Lars Kjaersgaard Hansen^a, Annette Rønholt Larsen^{a,c}, Henrik Petersenⁿ, Sönke Detlefsen^{b,c,d}

^a Hans Christian Andersen Children's Hospital, Odense University Hospital, Odense, Denmark

^b Odense Pancreas Center (OPAC), Odense University Hospital, Odense, Denmark

^c Institute of Clinical Research, University of Southern Denmark Odense, Odense, Denmark

^d Dept. of Pathology, Odense University Hospital, Odense, Denmark

^e Dept. of Paediatrics, Helsingborg Hospital, Sweden

^f The Kennedy Centre, Dept. of Clinical Genetics, Rigshospitalet, University of Copenhagen, Copenhagen, Denmark

^g Astrid Lindgren Children's Hospital, Karolinska University Hospital and Dept. of Women's and Children's Health, Karolinska Institutet, Stockholm, Sweden

^h Dept. of Clinical Genetics, Odense University Hospital, Denmark

ⁱ Dept. of Clinical Genetics, Skaane University Hospital, Lund, Sweden

^j Dept. of Paediatrics, Skaane University Hospital, Lund, Sweden

^k Dept. of Clinical Sciences, Lund University, Sweden

^l Dept. of Abdominal Surgery, Odense University Hospital, Denmark

^m Dept. of Pediatric Surgery, Skaane University Hospital, Lund, Sweden

ⁿ Dept. of Nuclear Medicine, Odense University Hospital, Odense, Denmark

ARTICLE INFO

Keywords:

Genome-wide uniparental disomy

Congenital hyperinsulinism

Beckwith-Wiedemann syndrome

Angelman syndrome

Mosaicism

ABSTRACT

Mosaic genome-wide paternal uniparental disomy (GW-pUPD) is a rarely recognised disorder. The phenotypic manifestations of multilocus imprinting defects (MLIDs) remain unclear. We report of an apparently non-syndromic infant with severe congenital hyperinsulinism (CHI) and diffuse pancreatic labelling by 18F*-DOPA-PET/CT leading to near-total pancreatectomy. The histology was atypical with pronounced proliferation of endocrine cells comprising > 70% of the pancreatic tissue and a small pancreatoblastoma. Routine genetic analysis for CHI was normal in the blood and resected pancreatic tissue. At two years' age, Beckwith-Wiedemann Syndrome (BWS) stigmata emerged, and at five years a liver tumour with focal nodular hyperplasia and an adrenal tumour were resected. pUPD was detected in 11p15 and next in the entire chromosome 11 with microsatellite markers. Quantitative fluorescent PCR with amplification of chromosome-specific DNA sequences for chromosomes 13, 18, 21 and X indicated GW-pUPD. A next generation sequencing panel with 303 SNPs on 21 chromosomes showed pUPD in both blood and pancreatic tissue. The mosaic distribution of GW-pUPD ranged from 31 to 35% in blood and buccal swap to 74% in the resected pancreas, 80% in a non-tumour liver biopsy, and 100% in the liver focal nodular hyperplasia and adrenal tumour. MLID features included transient conjugated hyperbilirubinaemia and lack of macrosomia from BWS (pUPD6); and behavioural and psychomotor manifestations of Angelman Syndrome (pUPD15) on follow-up. In conclusion, atypical pancreatic histology in apparently non-syndromic severe CHI patients may be the first clue to BWS and multi-syndromal CHI from GW-pUPD. Variations in the degree of mosaicism between tissues explained the phenotype.

1. Introduction

Beckwith-Wiedemann syndrome (BWS) most commonly occurs as a sporadic, genetic disorder with typical features such as macroglossia,

abdominal wall defects, lateralized overgrowth, visceromegaly, and increased risk of embryonal tumours (Weksberg et al., 2010; DeBaun et al., 2000; Brioude et al., 2018). Hypoglycaemia is reported in 30–50% of all newborns with BWS, usually resolving spontaneously

* Corresponding author. J.P. Windsloevs Vej 4, 5000, Odense C, Denmark.

E-mail address: henrik.christesen@rsyd.dk (H.T. Christesen).

¹ These authors contributed equally to this work.

<https://doi.org/10.1016/j.ejmg.2019.02.004>

Received 17 December 2018; Received in revised form 11 February 2019; Accepted 17 February 2019

Available online 21 February 2019

1769-7212/ © 2019 The Authors. Published by Elsevier Masson SAS. This is an open access article under the CC BY-NC-ND license (<http://creativecommons.org/licenses/by-nc-nd/4.0/>).

within the first month of life (Weksberg et al., 2010). However, a few patients suffer from severe and prolonged congenital hyperinsulinism (CHI) with hypoglycaemia necessitating intensive medical treatment and eventual near-total pancreatectomy (Brioude et al., 2018; Toda et al., 2017; Kalish et al., 2016). BWS is caused by various molecular defects affecting the imprinted growth regulatory genes within the 11p15 region in 80% (Li et al., 1998; Choufani et al., 2010). Most commonly, loss of methylation (LOM) of the imprinting centre *KCNQ1OT1* transcription start site differentially methylated region (*KCNQ1OT1*: TSS-DMR, previously known as imprinting centre 2 (IC2)) is seen, affecting the maternally imprinted genes *CDKN1C* (p57/Kip2) and *KCNQ1OT1*, followed by mosaic paternal uniparental disomy (pUPD). pUPD is routinely detected by LOM of *KCNQ1OT1*: TSS-DMR combined with gain of methylation (GOM) of the imprinting centre *H19/IGF2*: intergenic DMR (*H19/IGF2*: IG-DMR, previously known as imprinting centre 1 (IC1)), which enhances the expression of the paternally expressed growth promoter gene *IGF2* and reduces expression of maternally expressed and growth restraining *H19*. The combined effect of altered *H19/IGF2* expression cause increased growth as seen in BWS. (Choufani et al., 2010; Eggermann et al., 2016).

Non-syndromal CHI is most frequently caused by mutations of the K_{ATP} -channel genes *ABCC8* or *KCNJ11*, which are situated on 11p15 (Stanley, 2016). In the pancreas, a diffuse, a focal, and atypical histological forms are seen. The focal form is characterized by a paternal *ABCC8* or *KCNJ11* germline mutation combined with a somatic focal loss of maternal 11p15, usually in a very small area of the pancreas escaping conventional imaging, but detectable by 18F*-fluoro-dihydroxyphenylalanine (18F*-DOPA) PET/CT. In the focal lesion, imbalance of imprinted genes with expression of paternal growth promoter genes, but lack of expression of maternal tumour suppressor genes, results in overgrowth.

The histological features of the pancreas in BWS patients with prolonged, severe CHI have been sparsely described (Laje et al., 2013; Hussain et al., 2005). More recently, BWS patients with severe CHI were found to have mosaic, somatic pUPD extending to the adjacent K_{ATP} -channel genes on 11p15, unmasking an otherwise recessive, co-existing paternal K_{ATP} -channel mutation (Kalish et al., 2016; Kocaay et al., 2016; Calton et al., 2013). Rare BWS-spectrum patients show multilocus imprinting defects (MLIDs) with evidence of mosaic pUPD in other imprinted regions due to genome-wide pUPD (GW-pUPD), potentially including pUPD6 (low birth weight, conjugated hyperbilirubinaemia, transient neonatal diabetes); pUPD14 (Kagami-Ogata syndrome; psychomotor retardation, finger contractures, bell shaped thorax); pUPD15 (Angelman Syndrome) and pUPD20 (pseudohypoparathyroidism) (Wilson et al., 2008; Kalish et al., 2013). However, the phenotype correlation to MLIDs in BWS remains unclear (Brioude et al., 2018). Phenotypic variations are hypothesised to reflect differences in degree of mosaicism in different tissues and coexistence of paternal mutations with recessive presentation in the UPD paternal cell line (Wilson et al., 2008). To date, at least seven patients with GW-pUPD, BWS-features and CHI have been reported (Wilson et al., 2008; Kalish et al., 2013; Gogiel et al., 2013; Giurgea et al., 2006).

We report the case of a seemingly non-syndromic preterm infant with severe CHI and mosaic GW-pUPD without K_{ATP} -channel mutations, where follow-up revealed multi-syndromal CHI comprising BWS with abdominal tumours and features of pUPD6 and pUPD15/Angelman Syndrome.

2. Patient data

2.1. Clinical presentation at onset

The girl was the second child of healthy, non-related Caucasian parents. The pregnancy was naturally conceived and normal up to premature rupture of membranes and vaginal birth at gestational age 33 + 0 weeks in 2010. Birth weight was 2185 g (+0.2 SD), birth length

45 cm (+0.7 SD), head circumference 31.0 cm (+0.45 SD), Apgar score 9/1, 10/5, 10/10 min. No dysmorphic features were noted. She presented with blood glucose of 0.1 mmol/L at 2 h of age. The hypoglycaemia was promptly and adequately treated to avoid brain damage. Intravenous (i.v.) glucose demands reached 15 mg/kg/min despite simultaneous treatment with high doses of diazoxide, octreotide and i.v. glucagon. At glucose 2.2 mmol/L without medication, p-insulin was 105 (reference 12–77) pmol/L, C-peptide 4000 (reference 300–2400) pmol/L, confirming the diagnosis of hyperinsulinism. At blood glucose 4.1 mmol/L during i.v. 50% glucose infusion, p-insulin was haemolysed, but C-peptide was elevated to 2704 pmol/L and p-proinsulin was exceptionally high; > 260 (reference 2–23) pmol/L. To obtain normoglycemia, i.v. glucagon and i.v. glucose were required despite diazoxide and octreotide treatment. An 18F*-DOPA-PET/CT scan at 14 days of age showed DOPA uptake throughout the entire pancreas suggestive of diffuse congenital hyperinsulinism (Supplemental Fig. 1A). In retrospect, both the liver and the pancreas were enlarged compared to an age-matched patient with mild, diffuse CHI (Supplemental Fig. 1B). A near-total (90–95%) pancreatectomy was performed as early as at 20 days of age. Enlargement of the pancreas and liver was observed at surgery. By frozen section microscopy, diffuse hyperplasia of the islets of Langerhans was found. Information about immunohistochemical staining is listed in Supplementary Table 1.

2.2. Pancreatic histology and immunohistochemistry

The left-sided pancreatic resection specimen measured 10 × 20 × 70 mm. At microscopy, an increased number of endocrine cells, arranged in islets and small clusters, as well as single endocrine cells were observed throughout the pancreas (Fig. 1A). The endocrine cells occupied more than 70% of the parenchyma. All endocrine cells strongly expressed synaptophysin (Fig. 1B), and most of these cells were positive for insulin, while cells positive for glucagon and somatostatin were observed at the periphery of the islets. Acinar cells and small ducts were observed at the periphery of the pancreatic lobules and between the endocrine islets and cell clusters. When anti-p57/Kip2 was applied for immunohistochemistry, a positive reaction of varying intensity was seen in approximately 5% of the endocrine cells (Fig. 1C). The p57/Kip2-positive endocrine cells were mainly found in small hot spot areas. The exocrine tissue did not show any mentionable reaction. Control experiments applying the antibody to a focal type of CHI did not show expression of p57/Kip2. The entire resected pancreatic tissue showed these changes (Supplemental Fig. 2A). The proliferative activity assessed by Ki-67 was high, and the Ki-67 index reached 35% in hot spots. Compared with five randomly selected specimens from our archive of cases with the focal CHI, the density of nuclei in the endocrine lesion was 3.994 nuclei per 0.4 mm² in the BWS patient versus a mean of 2.513 nuclei per 0.4 mm² (range 1.759–3.544) in focal CHI.

In addition to the large endocrine lesion, a focus of pancreatoblastoma measuring 3 × 1 mm was noted (Supplemental Fig. 2B). Within the pancreatoblastoma, diffuse immunohistochemical expression of alfa-foetoprotein, cyclin D1 and cytokeratin CKA1/3 was found, and no expression of p63. Positivity for monoclonal carcinoembryonic antigen was seen in the columnar cells lining the duct-like structures. The squamoid nests in the pancreatoblastoma showed abnormal nuclear expression of beta-catenin. No overgrowth of exocrine tissue was observed.

2.3. Postoperative clinical course and BWS

Postoperative complications included transient hyperglycaemia, septicaemia, delayed establishment of enteral feeding, and transient malabsorption. An abnormally long-standing necrotic umbilical cord stump was resected at 41 days of age. The umbilicus was broad and slightly elevated, but without intestinal herniation into the cord stump,

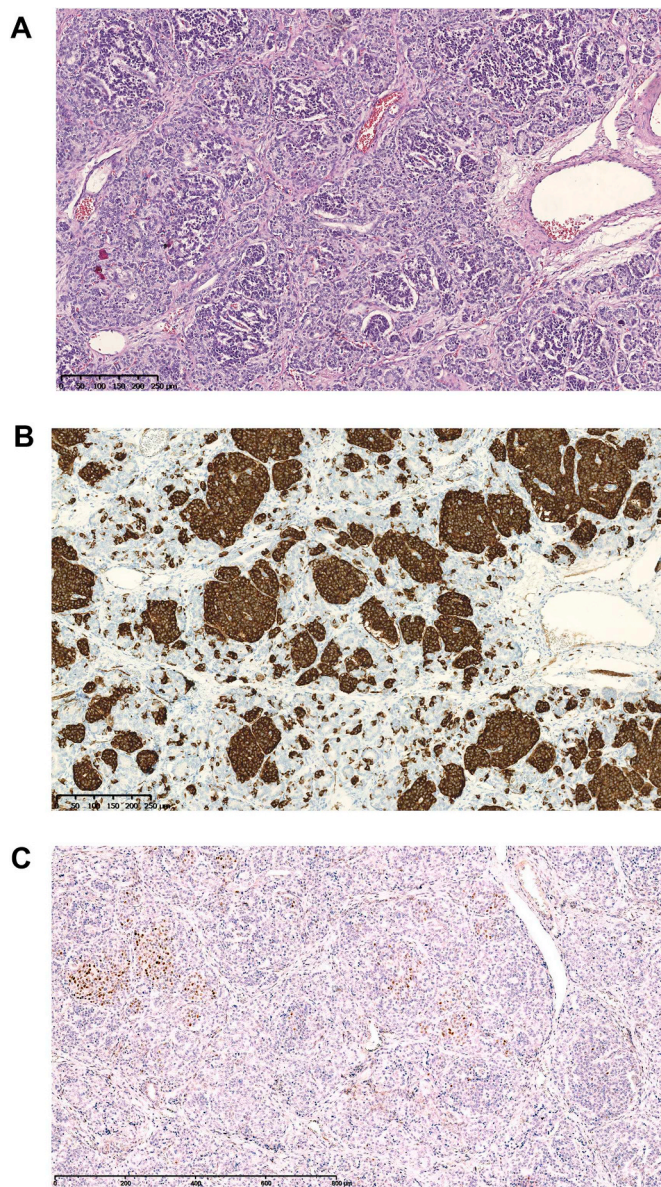


Fig. 1. Histological and immunochemical findings in pancreatic resection specimen from the patient. A) Increased numbers of endocrine cells arranged in islets and clusters are seen (H&E). B) Serial section of the area shown in A, demonstrating strong synaptophysin-positivity in the endocrine cells (synaptophysin immunostaining). C) The endocrine lesion showed expression of p57/Kip2 of varying intensity in approximately 5% of the endocrine cells, often found in small hot spot areas (p57/Kip2 immunostaining).

why BWS was not suspected.

From postoperative day 20, hypoglycaemia remitted, however milder. During diazoxide treatment, p-insulin was suppressed, 7 and 4 pmol/L, respectively, at blood glucose 3.0 and 2.9 mmol/L; C-peptide was in normal range, 188 and 202 pmol/L, but pro-insulin was still surprisingly high, 90 and 94 pmol/L. At follow-up until eight years of age, the hypoglycaemia was controlled with few exceptions of hypoglycaemia down to 2.8 mmol/L by diazoxide, long-acting release octreotide and dietary long carbohydrates. Fasting proinsulin levels were normalised along with p-insulin and C-peptide during treatment. Mild hypertrophic cardiomyopathy with mild aortic stenosis and mitral insufficiency were repeatedly found. Regarding syndromal features, BWS was suspected due to left-sided hemihypertrophy, enlarged

umbilicus without herniation, and enlarged liver by age two years. Repeat ultrasound investigations showed a hepatic process and a transient pseudocyst in the pancreas. Routine BWS screens for cancer were initially negative, but liver gamma glutamyl transferase was mildly elevated and a biopsy showed focal adenomatous hyperplasia (FNH) of the cystic liver process, which was resected at the age of 5½ years. The left kidney was enlarged, 11 cm long, with ill-defined border between the cortex and medulla, but without tumour. By MRI, a 3 cm right-sided adrenal tumour was found, leading to right-sided adrenalectomy at 6 years' age. By histology, the adrenal tumour had high mitotic activity, but uncertain potential of malignancy. The hemihypertrophy accounted for 1–2 cm increased leg length only at last follow-up. Height equalled 0 SD, weight +1SD.

3. Methods

Candidate gene analyses were in 2010 performed by denaturing high-performance liquid chromatography (dHPLC) with subsequent Sanger sequencing (Christesen et al., 2007). A subsequent next generation sequencing (NGS) CHI panel analysis was performed on blood and resected pancreatic tissue as previously described (Christiansen et al., 2018). Methylation analysis of the 11p15 locus was performed by MLPA (multiplex ligation-dependent probe amplification) analysis using kit ME030-C3 from MRC-Holland (MRC-Holland, Amsterdam, the Netherlands) following the manufacturer's instructions. The Coffalyser program (MRC-Holland) was used for data analysis.

Analysis for UPD of chromosome 11 was performed by microsatellite analysis using 12 polymorphic markers (D11S1363, D11S4046, D11S4146, D11S1760, D11S1338, D11S4149, D11S902, D11S4190, D11S915, D11S904, D11S917, D11S4090). A standard PCR reaction was performed using fluorescent tagged primers and taq gold polymerase. Products were analysed by capillary electrophoresis on an ABI3130XL (Applied Biosystems, Foster City, CA, USA) and the GeneMapper program (Applied Biosystems) were used for data analysis. Quantitative fluorescence (QF)–PCR using kit QST®Rplusv2 (Elucigene, Manchester, UK) comprising markers from chromosomes 13, 18, 21, X and Y was carried out on DNA from blood from the patient and both parents as an indication of GW-UPD. Furthermore, QF-PCR was performed on DNA from pancreatic tissue from the patient. DNA extracted from fresh liver (non-tumour and tumour) and adrenal tumour tissue was subjected to high resolution whole-genome genotyping using the CytoScan HD array (Thermo Fisher Scientific/Affymetrix) according to standard methods. The Chromosome Analysis Suite (ChAS, Thermo Fisher Scientific/Affymetrix) software was used to analyse CytoScan HD array data for B-allele frequency (BAF).

Sequencing was performed with a targeted NGS panel on blood, saliva and pancreatic tissue by use of the Agilent targeted sequence capture method followed by sequencing on the Illumina HiSeq1500 NGS platform (Illumina Inc, San Diego, CA). The sequencing design of the assay utilized designed oligonucleotides by use of Agilent SureDesign to capture all exons, 5'- and 3'-UTR, and 50 kb into the 5'- and 3'- UTR, and 50 kb into the flanking regions of the exons. A SureSelectXT Reagent kit (Agilent Technologies Denmark ApS, Glostrup, Denmark) was used and run on a single lane using paired-end sequencing at 2 × 100 bp. The covered region included 303 SNPs in 36 genes situated on chr. 1–14,16–19,20–22,X; among these 18 CHI/β-cell-related genes. The average coverage for the target regions was 127.7 reads.

The study was conducted in accordance with the Declaration of Helsinki and national guidelines. Permission to collect data from the patient record was acquired from the local Danish Research Ethics Committee (reference no. 54947). The project was approved by the Danish Data Protection Agency (journal no. 16/28242). The legal guardians of the patient approved publication.

4. Results

4.1. Genetic analyses

Before the pancreatic surgery, rapid genetic analysis and MLPA analysis of *ABCC8* and *KCNJ11* showed no indications of point mutations, deletions or duplications. Activating insulin gene sequence variants were initially suspected due to the extremely elevated p-proinsulin compared to p-insulin. However, postoperative dHPLC analysis showed no sequence variants affecting function in *INS*. Furthermore, no sequence variants affecting function were identified in the other CHI-genes *GLUD1*, *GCK*, *HNF1A*, *HNF4A*. In the later NGS panel analysis, no mutations were found in 18 CHI/ β -cell-related genes in the blood or pancreas, indicating no additional germline or somatic mutations related to CHI.

MLPA analysis for BWS showed LOM of *KCNQ1OT1*:TSS-DMR and GOM of *H19/IGF2*:IG-DMR thus confirming the BWS diagnosis. Since the conventional copy number MLPA analysis showed normal result, UPD was suspected as the genetic mechanism. This was confirmed by microsatellite analysis, which showed increased contribution of the paternal allele of six informative markers (six markers were non-informative; data not shown). Furthermore, whole chromosome 11 UPD was detected. QF-PCR analysis of chromosomes 13, 18, 21, and X in blood and pancreatic tissue indicated not only pUPD for chromosome 11, but GW-pUPD, Fig. 2. In blood, saliva and pancreatic tissue, pUPD was detected in 303 SNPs distributed on 21 chromosomes, Fig. 3. The mosaic distribution of GW-pUPD ranged from 31% in blood; 35% in buccal swap, to 74% in the resected pancreas; and by BAF analysis 80% in the non-tumour liver biopsy and 100% in the liver FNH and the adrenal tumour, Fig. 4 and Supplemental Fig. 3.

4.2. GW-pUPD phenotype correlations

Because of the mosaic GW-pUPD, we searched for other possible pUPD manifestations, including pUPD6, pUPD14, pUPD15, and pUPD20. Regarding pUPD6, transient conjugated hyperbilirubinaemia was noted in the neonatal period. The conjugated bilirubin peaked at 95 μ mol/L by age 18 days and the conjugated fraction reached a maximum of 71% (conjugated 68 μ mol/L, non-conjugated 28 μ mol/L) by age 37 days. By ultrasound, the bile ducts were not dilated. In the

right part of the liver, the bile duct tree was less visible compared to the left side, in retrospect suggesting segmental intrahepatic bile duct hypoplasia. No follow-up on this concern was done due to the transient nature of the clinical manifestations. Other pUPD6 features were not recorded, but may have been masked by the coexisting BWS with CHI. No finger contractures were seen and a chest X-ray aged five years showed normal configuration, which is why no indication of pUPD14 phenotype was present. Lastly, p-calcium and phosphate were normal, indicating that no pUPD20 phenotype was present.

Psychomotor and neurological examinations by five years of age showed a normal electroencephalogram and nerve conduction velocity test, global Motor ABC-score equalled the 75th percentile, but left-sided upper extremity ataxia was found and global balance score equalled the 25th percentile only. Fine motor score and ball skills equalled the 99.5th and 75th percentile, respectively. By standard paediatric neurological examination identified a slight suspicion of left-sided ankle spasticity and $\frac{1}{2}$ -1 year's retarded global psychomotor performance. Other clinical features compatible with Angelman Syndrome included short concentration span and hypermotoric behaviour, easy laughter, smile and joyousness, delayed language development, a very marked fascination of water, sleeping problems, heat intolerance and some degree of swallowing disturbance, but no facial, head or palmar dysmorfology. At latest follow-up eight years old, she was unable to read, although letters were recognised.

5. Discussion

We present an exceptional patient with severe, persistent CHI as the only presenting sign of BWS, remarkably elevated p-proinsulin levels, atypical histological pancreatic features with endocrine cells comprising more than 70% of the parenchyma and a congenital pancreatoblastoma. Mosaic GW-pUPD was identified with highest degree of 74–80% pUPD in the pancreas and non-tumour liver biopsy, to 100% in the liver FNH and the adrenal tumour. Clinical features of pUPD6 and pUPD15/Angelman Syndrome were detected compatible with GW-pUPD.

The phenotype of mosaic somatic gene alterations is expected to vary according to the degree of mosaicism in affected tissue. Mosaicism is especially frequent in the imprinting disorders of 11p15, BWS and Silver-Russell Syndrome (Mackay and Temple, 2017). A broader

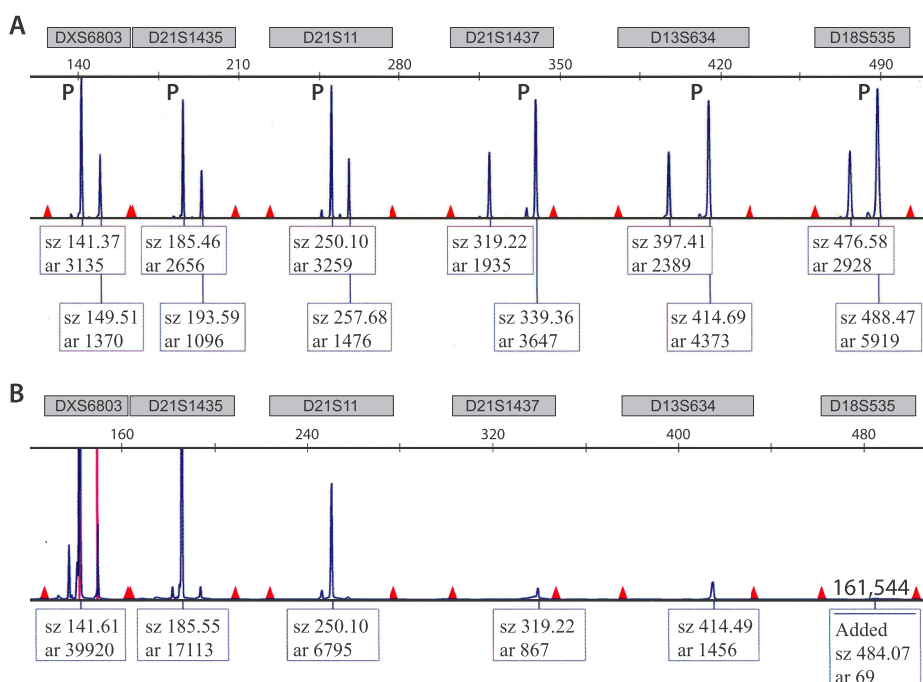


Fig. 2. QF-PCR analysis on DNA from blood and pancreatic tissue indicating GW-pUPD. A) QF-PCR analysis of DNA from blood. Only a subset of markers is shown, one marker located on the X-chromosome (DXS6803), one marker located on chromosome 13 (D13S634), one marker from chromosome 18 (D18S535) and three markers from chromosome 21 (D21S1435, D21S11, D21S1437). Alleles marked with a "P" indicate the paternal allele. B) QF-PCR analysis of DNA from pancreas tissue. The same six markers are shown. Only the paternal allele appears in DNA from pancreas tissue.

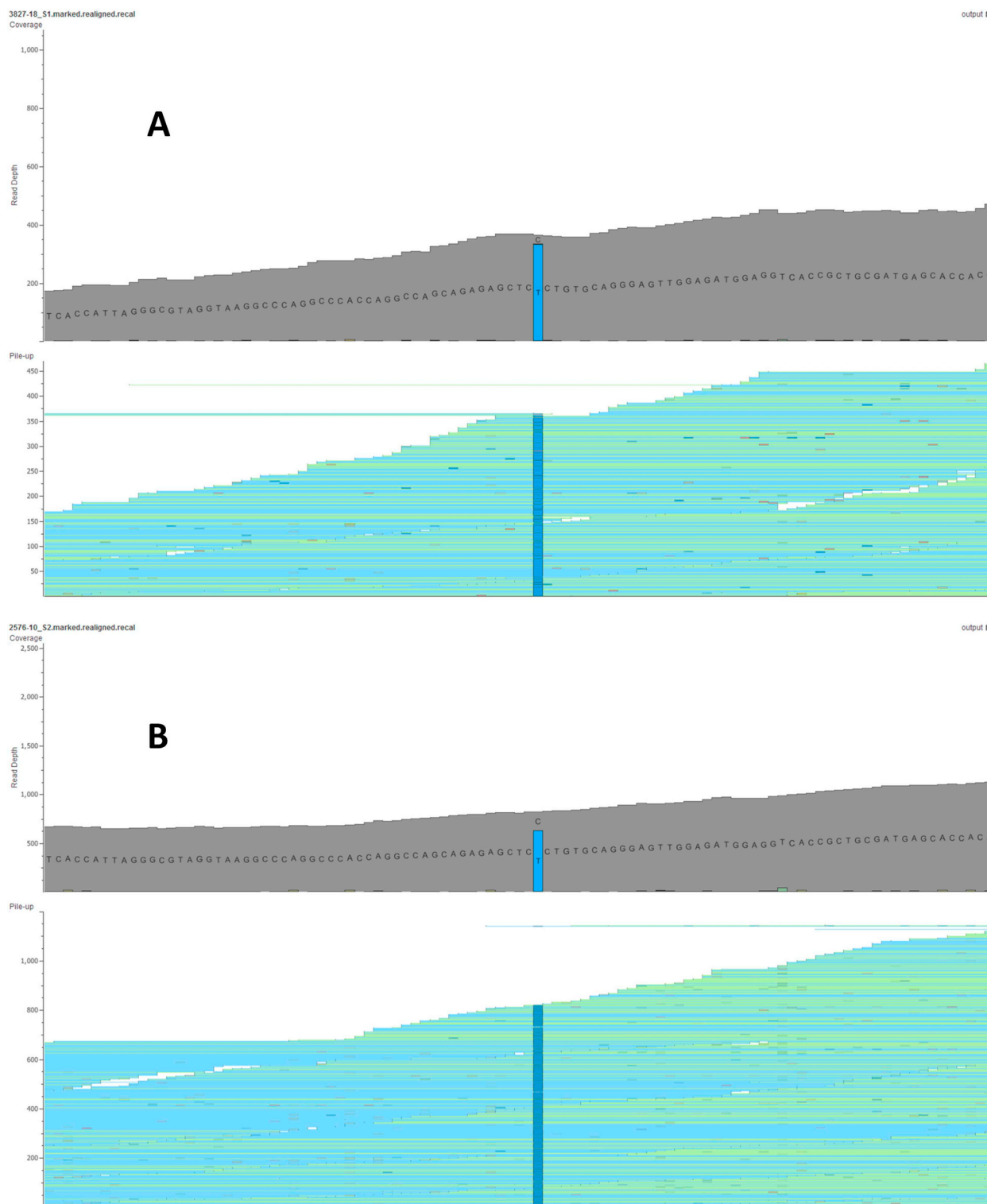


Fig. 3. Direct sequencing of 303 SNPs on 21 chromosomes in DNA from pancreatic tissue and blood, exemplified by the *ABCC8* SNP rs1799859. NGS sequencing of DNA by coverage (on top) and read pile-up (bottom) from formalin-fixed parafin-embedded pancreatic tissue (A) and blood (B). The mosaic distribution of GW-pUPD was 74% in the pancreas and 31% in the blood.

spectrum of BWS (BWSp) from isolated lateralized overgrowth to classical BWS is now recognised, partly caused by variations in somatic mosaicism (Brioude et al., 2018).

In BWS with CHI, pUPD has been found in most (26/28) patients (Kalish et al., 2016), in contrast to approximately 20% in BWS in general. When not associated with additional CHI-related gene mutations, pancreatic islet cell overgrowth is suggested to be the

pathophysiological mechanism of the hyperinsulinism. However, this has been regarded to lead to mild CHI only, in contrast to patients with BWS *plus* a K_{ATP} -channel mutation (Kalish et al., 2016; Kocaay et al., 2016). Our patient had no additional germline or somatic CHI gene mutations, but a high mosaic degree of pUPD in the resected pancreas. Moreover, a high β -cell number in the pancreas and an extremely increased p-proinsulin compared to p-insulin showed evidence of severe

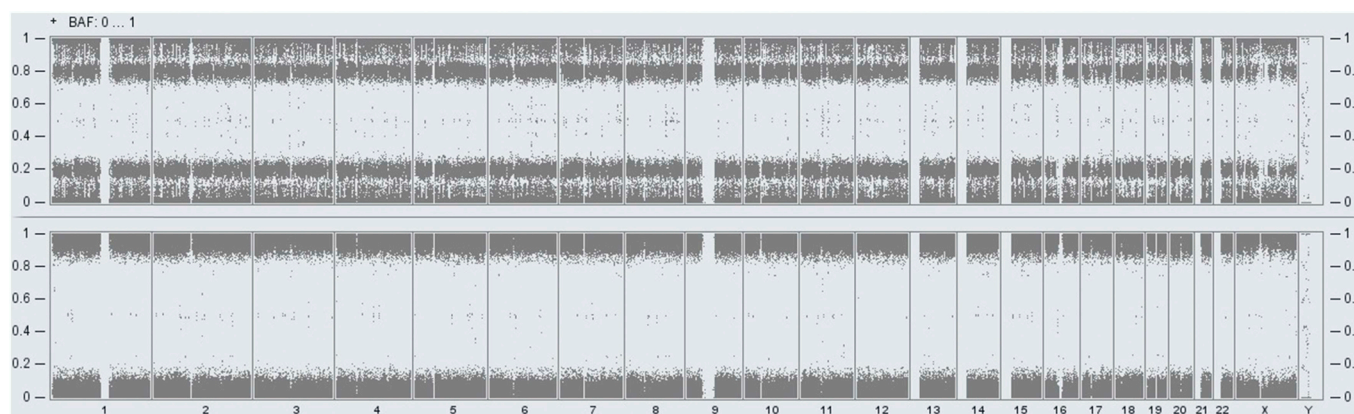


Fig. 4. B-allele frequency (BAF) profiles along all chromosomes obtained by genomic array. Upper panel: The BAF-profile reveals mosaic genome-wide loss of heterozygosity in a non-neoplastic liver sample of the patient. Mosaic BAF lines are seen around 0.8 and 0.2. Lower panel: The BAF-profile of a neoplastic liver biopsy from the patient with genome wide loss of heterozygosity in the tumour cells, suggesting that the neoplasia has arisen from a cell with GW-pUPD.

hyperinsulinism due to β -cell overgrowth with hyperproduction of proinsulin. Likewise, disproportionate hyperproinsulinaemia is a characteristic finding in insulinoma patients with loss-of-function mutations in the tumour suppressor gene *MEN1* (Vezzosi et al., 2007). In contrast, CHI from K_{ATP} -channel mutations typically shows insulin hypersecretion, evidenced by a relative lower proinsulin:insulin ratio (Christesen et al., 2001).

Severe neonatal CHI as the only presenting feature in BWS has to our knowledge only been described once before by Hussain et al. (2005), but in less details. In the report by Hussain et al., severe CHI was seen and the β -cell K_{ATP} -channel function was altered despite no detected mutations in *ABCC8* or *KCNJ11*. A search for somatic K_{ATP} -channel mutations was, however, not performed. Adachi et al. reported a BWS patient with severe CHI and macrosomia from birth as the only BWS features (Adachi et al., 2013). In the Kalish et al. cohort of BWS in CHI patients, additional BWS stigmata were found in all patients at birth. The number of BWS stigmata correlated significantly with the mosaic percentage of pUPD in the blood (Kalish et al., 2016). In our patient, the low variable mosaic degree of pUPD from 31 to 35% in the blood and saliva to 74–100% in the pancreas, liver FNH and adrenal tumour correlated well with the phenotype. The hypertrophic cardiomyopathy is a common finding in CHI as a result of the anabolic effect of foetal hyperinsulinism (Huang et al., 2013).

The pancreatic histology was atypical with some features reminiscent of both focal and diffuse CHI (Rahier et al., 2011; Ismail et al., 2012; Kloppel et al., 1999). In contrast to focal CHI, our patient showed increased endocrine cells throughout the pancreas in extreme numbers, but did not show the typical confluence of islets of Langerhans often seen in classical focal CHI. Furthermore, expression of p57/Kip2 was seen in approximately 5% of the endocrine cells in contrast to focal CHI, where loss of maternal 11p15 leads to total absence of p57 expression in the lesion. Our findings are probably similar to the atypical histological changes reported in less details in a few other BWS patients with CHI (Laje et al., 2013; Hussain et al., 2005). Of note, the association of an atypical endocrine pancreatic lesion at histology together with a congenital pancreatoblastoma as in our patient has only been reported once before (Laje et al., 2013), but may serve as a clue for BWS.

At follow-up, our patient developed BWS features and characteristic abdominal tumours. Both CHI and abdominal tumours are seemingly more frequent in the 14 reported BWS patients with GW-pUPD to date (Wilson et al., 2008; Kalish et al., 2013; Inbar-Feigenberg et al., 2013; Bertoin et al., 2015). Our finding of a skewed allele distribution with 74–100% pUPD in the resected pancreatic, liver and adrenal tissue indicated that the hyperinsulinism and abdominal tumours reflected the high degree of pUPD11, rather than other pUPD manifestations in these

tissues. It can be speculated that GW-pUPD patients are prone to a higher degree of skewed allele distribution in abdominal tissues compared to patients with BWS due to pUPD11.15 alone. Consistent with the concept of GW-pUPD, where an androgenic 46, XY lineage is lethal (Yamazawa et al., 2011), our and all other published patients were females.

As resumed by Kalish et al. (2013), a few GW-pUPD BWS patients display features of other syndromes associated with paternal UPD for other chromosomes, notably UPD14, UPD15, UPD6 and UPD20. Due to mosaicism, a phenotypic spectrum is to be expected. We found clear behavioural and developmental features which could be associated with pUPD15/Angelman Syndrome already at five years of age. We did not assign any of these features with neurological complications to hypoglycaemia, as this was prompt and adequately treated; neither to the late preterm birth. One other study mentioned poor language and unsteady gait as Angelman features in a 13-y-old girl with GW-pUPD and BWS, CHI and 25% mosaicism for pUPD15 (Inbar-Feigenberg et al., 2013), but no other Angelman features, and the cerebral damage due to severe hypoglycaemia at birth was not discussed as an alternative cause.

Lastly, transient neonatal conjugated hyperbilirubinaemia and suspicion of segmental intrahepatic bile duct hypoplasia were found in our patient, compatible with pUPD6 (Kenny et al., 2009). Other features of pUPD6 include low birth weight and transient neonatal diabetes. It is likely that these features were counterbalanced by the BWS with CHI phenotype, resulting in normal birth weight and hypoglycaemia, leaving conjugated hyperbilirubinaemia as the only clear manifestation of pUPD6.

In conclusion, GW-pUPD may present with severe CHI as the only clear manifestation at birth, but with overt BWS including abdominal tumours and features of pUPD6 (conjugated hyperbilirubinaemia) and pUPD15 (Angelman Syndrome) at follow-up. The degree of mosaic pUPD ranged from 31 to 35% in the blood to 74–100% in the resected pancreas and adrenal and liver tumour, demonstrating that the phenotype of GW-pUPD depends on tissue-variations in the degree of mosaicism. In unexplained, seemingly non-syndromal severe CHI, identification of pUPD11p15 (both sexes) and eventual GW-pUPD (girls only) will provide a basis for appropriate clinical follow-up regarding emerging multi-syndromal features. We introduce the novel name multi-syndromal CHI to shortly describe GW-pUPD with CHI as the dominant and presenting feature. In patients with clinical suspicion of multi-syndromal CHI, GW-pUPD analyses should be performed.

Conflicts of interest

The authors declare no conflicts of interest.

Funding

This research did not receive any specific grant from funding agencies in the public, commercial, or non-for-profit sectors.

Acknowledgements

The authors wish to thank the parents and numerous hospital staff members for their clinical contributions at hospitals in Helsingborg, Lund and Göteborg, Sweden and Odense, Denmark. No funding was linked to this manuscript.

Appendix A. Supplementary data

Supplementary data to this article can be found online at <https://doi.org/10.1016/j.ejmg.2019.02.004>.

References

- Adachi, H., et al., 2013. Congenital hyperinsulinism in an infant with paternal uniparental disomy on chromosome 11p15: few clinical features suggestive of Beckwith-Wiedemann syndrome. *Endocr. J.* 60 (4), 403–408.
- Bertoin, F., et al., 2015. Genome-wide paternal uniparental disomy as a cause of Beckwith-Wiedemann syndrome associated with recurrent virilizing adrenocortical tumors. *Horm. Metab. Res.* 47 (7), 497–503.
- Brioude, F., et al., 2018. Expert consensus document: clinical and molecular diagnosis, screening and management of Beckwith-Wiedemann syndrome: an international consensus statement. *Nat. Rev. Endocrinol.* 14 (4), 229–249.
- Calton, E.A., et al., 2013. Hepatoblastoma in a child with a paternally-inherited ABCC8 mutation and mosaic paternal uniparental disomy 11p causing focal congenital hyperinsulinism. *Eur. J. Med. Genet.* 56 (2), 114–117.
- Choufani, S., Shuman, C., Weksberg, R., 2010. Beckwith-Wiedemann syndrome. *Am. J. Med. Genet. C Semin. Med. Genet.* 154c (3), 343–354.
- Christesen, H.B., Feilberg-Jorgensen, N., Jacobsen, B.B., 2001. Pancreatic beta-cell stimulation tests in transient and persistent congenital hyperinsulinism. *Acta Paediatr.* 90 (10), 1116–1120.
- Christesen, H.B., et al., 2007. Rapid genetic analysis in congenital hyperinsulinism. *Horm. Res.* 67 (4), 184–188.
- Christiansen, C.D., et al., 2018. 18F-DOPA PET/CT and 68Ga-DOTANOC PET/CT scans as diagnostic tools in focal congenital hyperinsulinism: a blinded evaluation. *Eur. J. Nucl. Med. Mol. Imaging* 45 (2), 250–261.
- DeBaun, M.R., King, A.A., White, N., 2000. Hypoglycemia in Beckwith-Wiedemann syndrome. *Semin. Perinatol.* 24 (2), 164–171.
- Eggermann, K., et al., 2016. EMQN best practice guidelines for the molecular genetic testing and reporting of chromosome 11p15 imprinting disorders: Silver-Russell and Beckwith-Wiedemann syndrome. *Eur. J. Hum. Genet.* 24 (10), 1377–1387.
- Giurgea, I., et al., 2006. Congenital hyperinsulinism and mosaic abnormalities of the ploidy. *J. Med. Genet.* 43 (3), 248–254.
- Gogiel, M., et al., 2013. Genome-wide paternal uniparental disomy mosaicism in a woman with Beckwith-Wiedemann syndrome and ovarian steroid cell tumour. *Eur. J. Hum. Genet.* 21 (7), 788–791.
- Huang, T., et al., 2013. Hypertrophic cardiomyopathy in neonates with congenital hyperinsulinism. *Arch. Dis. Child. Fetal Neonatal Ed.* 98 (4), F351–F354.
- Hussain, K., et al., 2005. Hyperinsulinemic hypoglycemia in Beckwith-Wiedemann syndrome due to defects in the function of pancreatic beta-cell adenosine triphosphate-sensitive potassium channels. *J. Clin. Endocrinol. Metab.* 90 (7), 4376–4382.
- Inbar-Feigenberg, M., et al., 2013. Mosaicism for genome-wide paternal uniparental disomy with features of multiple imprinting disorders: diagnostic and management issues. *Am. J. Med. Genet.* 161 (1), 13–20.
- Ismail, D., et al., 2012. The heterogeneity of focal forms of congenital hyperinsulinism. *J. Clin. Endocrinol. Metab.* 97 (1), E94–E99.
- Kalish, J.M., et al., 2013. Clinical features of three girls with mosaic genome-wide paternal uniparental isodisomy. *Am. J. Med. Genet.* 161a (8), 1929–1939.
- Kalish, J.M., et al., 2016. Congenital hyperinsulinism in children with paternal 11p uniparental isodisomy and Beckwith-Wiedemann syndrome. *J. Med. Genet.* 53 (1), 53–61.
- Kenny, A.P., et al., 2009. Concurrent course of transient neonatal diabetes with cholestasis and paucity of interlobular bile ducts: a case report. *Pediatr. Dev. Pathol.* 12 (5), 417–420.
- Kloppel, G., Reinecke-Luthge, A., Koschoreck, F., 1999. Focal and diffuse beta cell changes in persistent hyperinsulinemic hypoglycemia of infancy. *Endocr. Pathol.* 10 (4), 299–304.
- Kocaay, P., et al., 2016. Coexistence of mosaic uniparental isodisomy and a KCNJ11 mutation presenting as diffuse congenital hyperinsulinism and hemihypertrophy. *Horm. Res. Paediatr.* 85 (6), 421–425.
- Laje, P., et al., 2013. Pancreatic surgery in infants with Beckwith-Wiedemann syndrome and hyperinsulinism. *J. Pediatr. Surg.* 48 (12), 2511–2516.
- Li, M., Squire, J.A., Weksberg, R., 1998. Overgrowth syndromes and genomic imprinting: from mouse to man. *Clin. Genet.* 53 (3), 165–170.
- Mackay, D.J.G., Temple, I.K., 2017. Human imprinting disorders: principles, practice, problems and progress. *Eur. J. Med. Genet.* 60 (11), 618–626.
- Rahier, J., Guiot, Y., Sempoux, C., 2011. Morphologic analysis of focal and diffuse forms of congenital hyperinsulinism. *Semin. Pediatr. Surg.* 20 (1), 3–12.
- Stanley, C.A., 2016. Perspective on the genetics and diagnosis of congenital hyperinsulinism disorders. *J. Clin. Endocrinol. Metab.* 101 (3), 815–826.
- Toda, N., et al., 2017. Hyperinsulinemic hypoglycemia in Beckwith-Wiedemann, Sotos, and Kabuki syndromes: a nationwide survey in Japan. *Am. J. Med. Genet.* 173 (2), 360–367.
- Vezzosi, D., et al., 2007. Insulin, C-peptide and proinsulin for the biochemical diagnosis of hypoglycaemia related to endogenous hyperinsulinism. *Eur. J. Endocrinol.* 157 (1), 75–83.
- Weksberg, R., Shuman, C., Beckwith, J.B., 2010. Beckwith-Wiedemann syndrome. *Eur. J. Hum. Genet.* 18 (1), 8–14.
- Wilson, M., et al., 2008. The clinical phenotype of mosaicism for genome-wide paternal uniparental disomy: two new reports. *Am. J. Med. Genet.* 146a (2), 137–148.
- Yamazawa, K., et al., 2011. Androgenetic/biparental mosaicism in a girl with Beckwith-Wiedemann syndrome-like and upd(14)pat-like phenotypes. *J. Hum. Genet.* 56 (1), 91–93.